# SIMULATION OF HIGH REYNOLDS NUMBER FLOW FOR AERODYNAMIC DESIGN: THREE DECADES IN THE REARVIEW MIRROR AND THE ROAD AHEAD.

PRINCETON UNIVERSITY

*Luigi Martinelli*

# Outline

I. A look back at some of the advances made over 15 years ('84 – '99) in and around the MAE Department or more precisely my incredible life journey with Antony

II. A path forward.

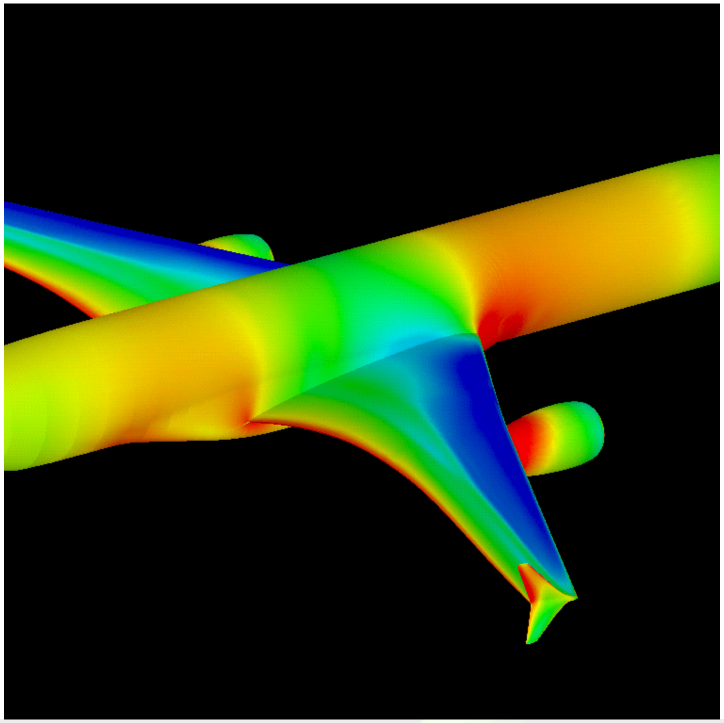

# The Beginning

Summer 1984: I joined Antony's group

Assigned Reading of

Transonic Flow Calculations, Princeton University Report MAE 1651, March 1984, in Numerical Methods in Fluid Dynamics, edited by F. Brezzi, Lecture Notes in Mathematics, Vol. 1127, Springer-Verlag, 1985, pp. 156-242.

Departure point for research

Development of a Navier-Stokes Method Based on a Finite Volume Technique for the Unsteady Euler Equations (with W. Haase and B. Wagner), Proceedings of 5th GAMM Conference on Numerical Methods in Fluid Mechanics, Rome, Italy, October 1983.

Assignment: Demonstrate the Multigrid Time stepping scheme for RANS

# Steady State Solvers Built on Time Evolution

$$\frac{dw}{dt} + R(w) = 0$$

Explicit methods facilitate vector and parallel processing

Lax- Wendroff

Steady state depend on the time step

Multistage

- Integrate the time dependent equations until a steady state.
- The true time dependent equations reach a steady state very slowly
- Modify equations in order to accelerate the evolution to the steady state.

# Multigrid Time Stepping

The underlying idea of a multigrid time stepping scheme is to transfer some of the task of tracking the evolution of the system to a sequence of successively coarser meshes.

Advantages.

The use of larger control volumes on the coarser grids tracks the evolution on a larger scale, with the consequence that global equilibrium can be more rapidly attained.

In the case of an explicit time stepping scheme, this manifests itself through the possibility of using successively coarse meshes, without violating the stability bound.

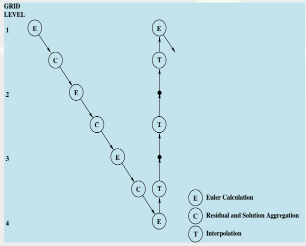


Special transfer operations need to be defined. First the solution vector on grid $k$ must be initialized as

$$\mathbf{w_k^{(0)}} = T_{k,k-1}\mathbf{w_{k-1}} \tag{1}$$

where $\mathbf{w_{k-1}}$ is the current value on grid $k-1$, and $T_{k,k-1}$ is a transfer operator. Next it is necessary to transfer a residual forcing function such that the solution on grid $k$ is driven by the residuals calculated on grid $k-1$. This can be accomplished by setting

$$\mathbf{P_k} = Q_{k,k-1}\mathbf{R_{k-1}}(\mathbf{w_{k-1}}) - \mathbf{R_k}(\mathbf{w_k^{(0)}}) \tag{2}$$

where $Q_{k,k-1}$ is another transfer operator.
Then $\mathbf{R_k}(\mathbf{w_k})$ is replaced by $\mathbf{R_k}(\mathbf{w_k}) + \mathbf{P_k}$ in the time stepping scheme.
Finally one sets

$$\mathbf{w_{k-1}^+} = \mathbf{w_{k-1}} + I_{k-1,k}\left(\mathbf{w_k^+} - \mathbf{w_k^0}\right) \tag{3}$$

where $w_{k-1}$ is the solution on grid $k-1$ after the time step on grid $k-1$ and before the transfer from grid $k$, and $I_{k-1,k}$ is an interpolation operator.

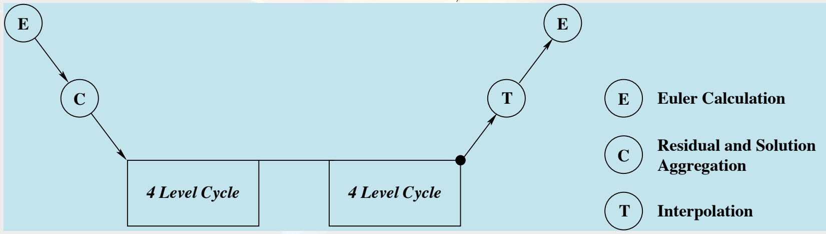

# Barriers

**In house Computational Resources.**

IBM 4341 ➔ Masscomp ➔ Celerity

Laminar Calculation (Low Reynolds)

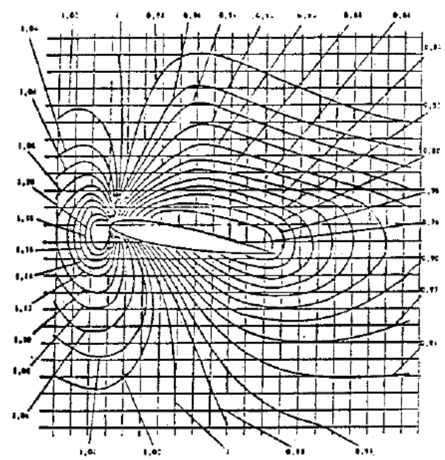

*Fig.* 5.2.18
NACA 0012 airfoil -
Experimental Density Contours

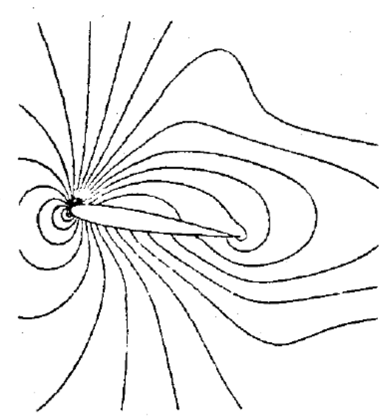

*Fig.* 5.2.19
NACA 0012 airfoil -
Computed Density Contours ($D\rho = .05$)

**Grid generation for highly stretched viscous meshes.**

Ultimately they were both overcome with the help of Paul Rubbert's group at Boeing who hosted me in December of 1985 for a month and allowed me access to their Cray XMP, and Larry Wigton's hyperbolic grid generator.

# Lesson Learned

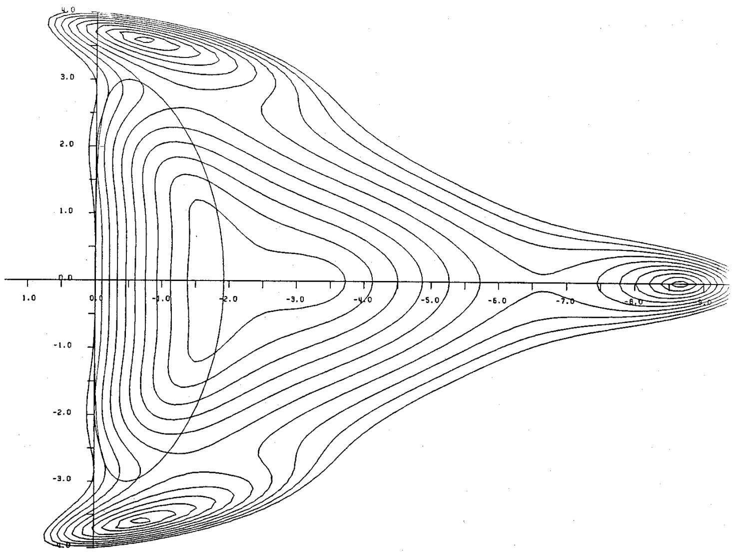

*Fig.* 3.5.2
Stability region of the five stage scheme
with three evaluations of dissipation.
Contour lines $\Delta |f(z)| = .1$
and locus of $z(\xi)$ for $\lambda = 3.0$, $\mu = 1/32$
in the complex z-plane ( $z = -i\lambda \sin\xi - 4\lambda\mu(1-\cos\xi)^2$ ) .

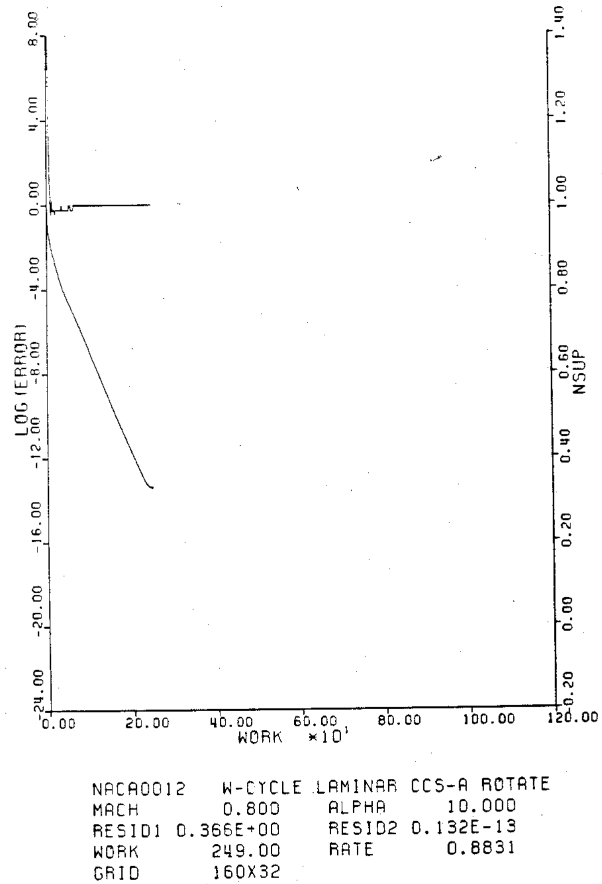


Care must be taken to counteract the negative
Effects of high aspect ratio meshes

# Conclusions from my thesis - 1987

In this work the finite volume formulation has been extended to the treatment of the compressible two dimensional Navier Stokes equations for both cell centered and vertex schemes on regular quadrilateral meshes. Two alternative discretization formulas for the cell centered schemes have been evaluated.

same turbulence model. For attached flows good agreement with experimental data is also obtained. When the shock boundary layer interaction becomes strong enough to cause significant separation the algebraic turbulence models fails to produce a good simulation, and large variations in the results can be produced by substituting alternative models. Alternative application of

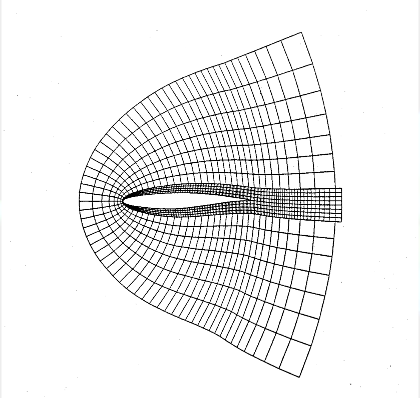

tion and use of appropriate preconditioning [71]. It has been noted in this study that one of the main constraints on the time step limit of our explicit scheme for viscous computations is the limit set by the wave speed in the inner region of the boundary layer. This constraint comes about because of the 'hyperbolic' treatment of the convection operator everywhere in the flow field. However, there are large regions within the boundary layer where the flow is locally incompressible. Optimization of the scheme in these regions could be achieved by sacrificing time accuracy in favor of the introduction of an appropriate preconditioning matrix.

# 3D - Solvers

- Mohan Jayaram  first effort to extend FLO57
- Veer Vatsa  extension of FLO57  at Langley
- Feng Liu Ph.D. work  with emphasis on turbomachinery
- Antony's work with H. Rieger on LU schemes.

- Ultimately AJ and LM re-wrote both single block cell centered (**Flo107**)  and cell vertex formulation **(Flo97**).
- '93 – '94 LM developed  a multiblock version **Flo107-MB** which was initially debugged by J. Farmer and later parallelized by J.J. Alonso.

Multigrid Navier-Stokes Calculations for Three Dimensional Cascades, F. Liu and A. Jameson, AIAA Paper 92-0190, AIAA 30th Aerospace Sciences Meeting, Reno, January 1992 and AIAA Journal 1993, Vol. 31, No. 10, pp. 1785-1791.

Numerical Simulation of Three-Dimensional Vortex Flows over Delta Wing Configurations, L. Martinelli, E. Malfa, A. Jameson, Proceedings of the 13th International Conference on Numerical Methods in Fluid Dynamics, Rome, July 1992.

# Game Changers - I

- Jameson Local Extremum Diminishing Theory: SLIP – USLIP construction (1994)

Design, Implementation, and Validation of Flux Limited Schemes for the Solution of the Compressible Navier-Stokes Equations, S. Tatsumi, L. Martinelli and A. Jameson AIAA Paper 94-0647, AIAA 32nd Aerospace Sciences Meeting and Exhibit, Reno, January 1994; Flux Limited Schemes for the Solution of the Compressible Navier-Stokes Equations, AIAA Journal, Vol. 33, No. 2, pp. 252-261, February 1995 S. Tatsumi , L. Martinelli and Jameson.

A New High Resolution Scheme for Compressible Viscous Flows with Shocks ,S. Tatsumi, L. Martinelli and A. Jameson, AIAA Paper 95-0466, AIAA 33rd Aerospace Sciences Meeting and Exhibit, Reno, January 1995.

# Shock Capturing

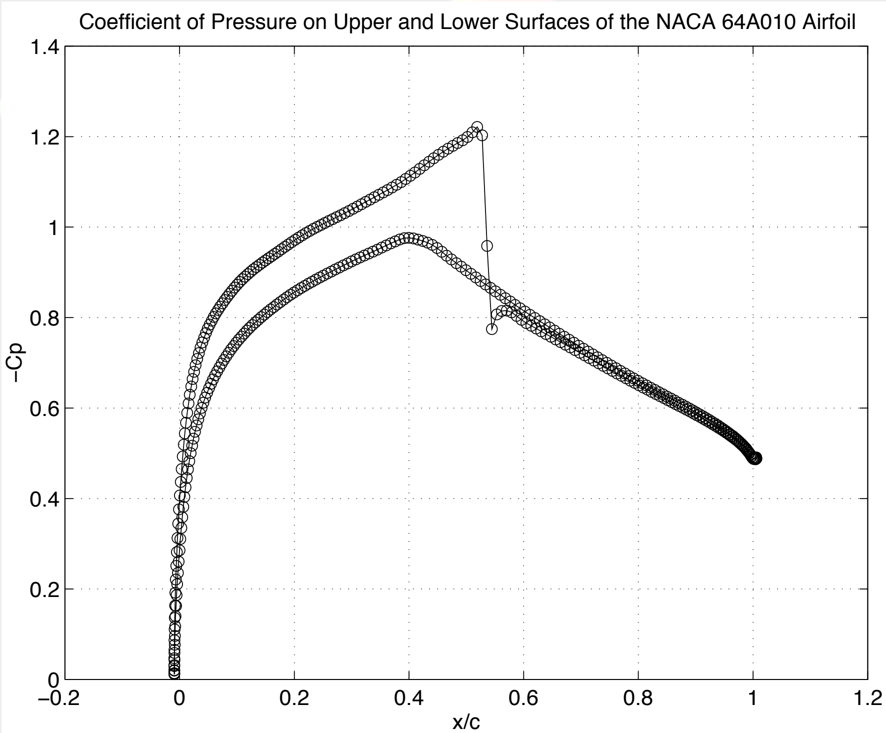


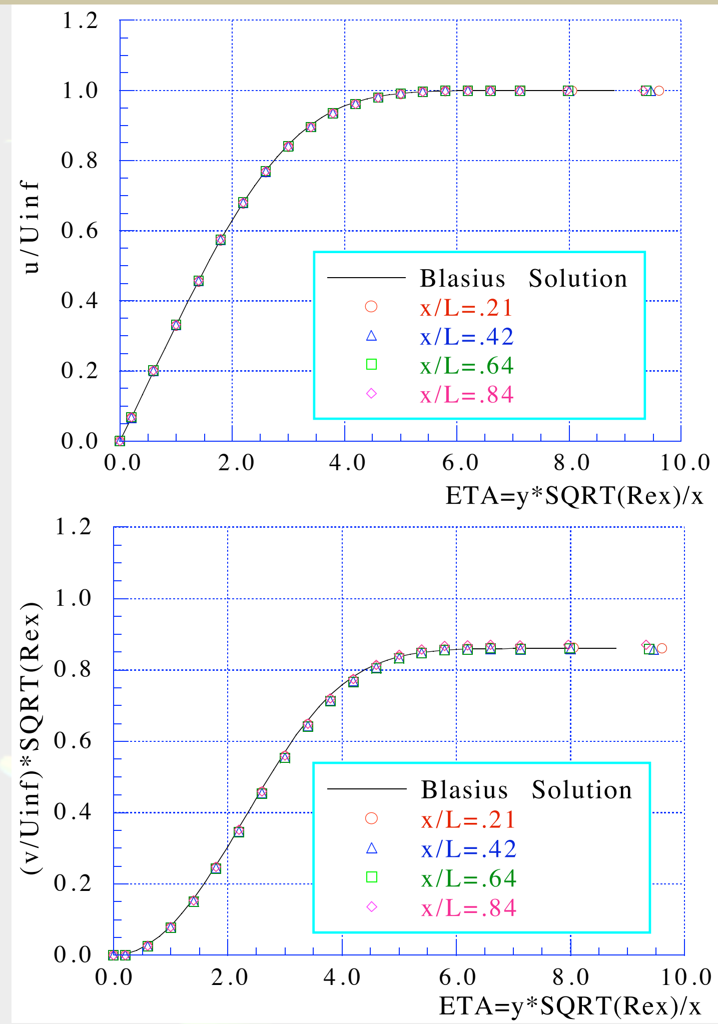


Convective Upstream Split Pressure (CUSP) With ELED Limiter.

# Game Changers - II

◆ IBM – SP system provided us with a quantum leap in the computational Power available, thus enabling us to attack several more complex problems, including time-resolved flow.

J.J. Alonso took the lead on developing parallelization strategies for the **Flo-**codes using an SPMD approach.

A Two-Dimensional Multigrid Navier-Stokes Solver for Multiprocessor Architectures, J.J. Alonso, T.J. Mitty, L. Martinelli, and A. Jameson. Proceedings of Parallel CFD '94, Kyoto, May 1994, Parallel Computational Fluid Dynamics: New Algorithms and Applications (ed. Satofuka, Periaux ), Elsevier Science B.V., 1995.

Time Dependent Calculations Using Multigrid, with Applications to Unsteady Flows Past Airfoils and Wings, A. Jameson ,AIAA Paper 91-1596, AIAA 10th Computational Fluid Dynamics Conference, Honolulu, June 1991.

The idea is to use an implicit scheme with a large stability region (A-stable or stiffly stable) and to solver the implicit equations at each time step by inner iterations using an accelerated time evolution scheme in artificial time. The second order BDF is

$$\frac{3}{2\Delta t}w^{n+1} - \frac{2}{\Delta t}w^{n} + \frac{1}{2\Delta t}w^{n-1} + R(w^{n+1}) = 0 \tag{1}$$

With dual time stepping solve

$$\frac{dw}{dt^*} + \frac{3}{2\Delta t}w - \frac{2}{\Delta t}w^{n} + \frac{1}{2\Delta t}w^{n-1} + R(w) = 0 \tag{2}$$

in pseudo time $t^*$ to reach a steady state satisfying equation (2).

Multigrid Unsteady Navier-Stokes Calculations with Aeroelastic Application, J. Alonso, L. Martinelli, A. Jameson. AIAA Paper 95-0048, AIAA 33rd Aerospace Sciences Meeting and Exhibit, Reno, January 1995.

# RANS Results Using FLO107-MB For Drag Prediction Workshop

Statistical Evaluation DPW1 – All Participants

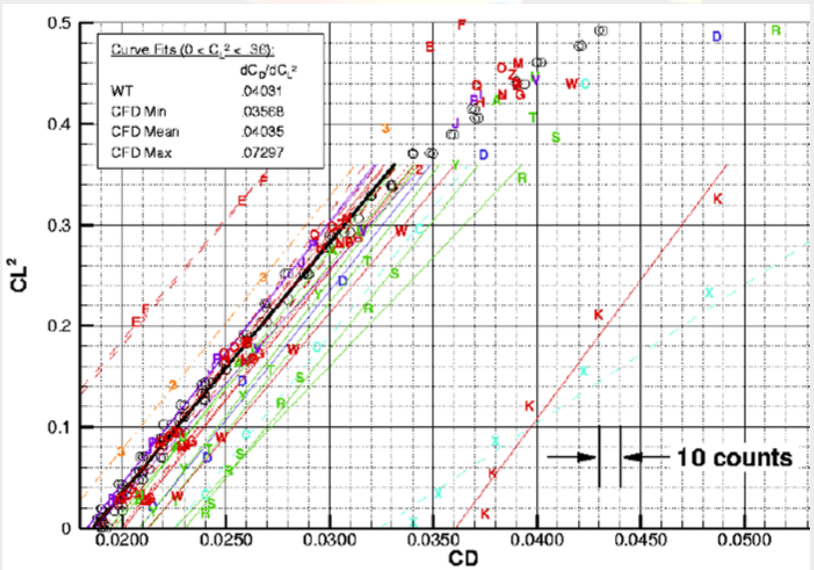


Flo107-MB (DPW2)

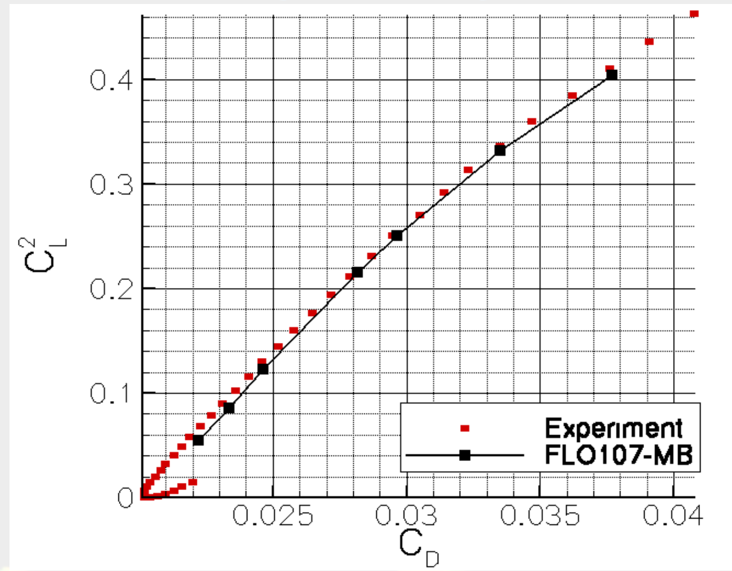


- Accurate drag prediction for complex geometries in transonic flow is still very hard
- FLO107-MB has been thoroughly validated.
- Results of right figure were obtained with CUSP scheme and k -$\omega$ turbulence model

# RANS Results for DPW-V
# Medium Mesh

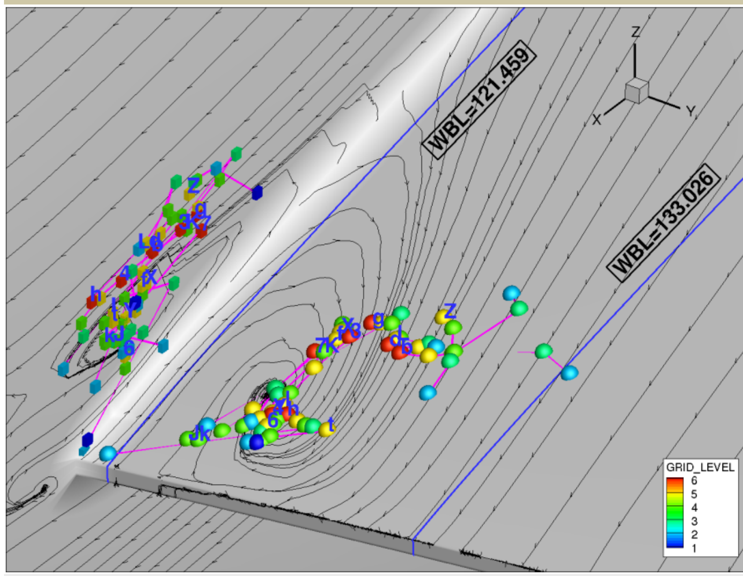


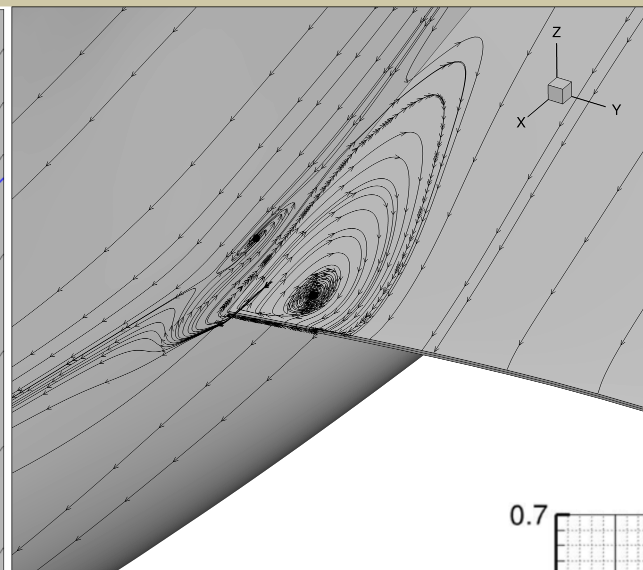


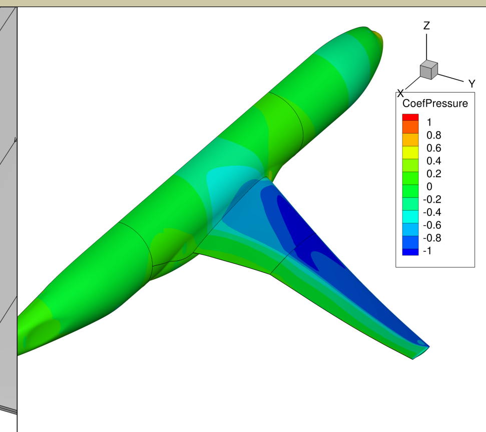


Good correlation with experimental
Data (corrected)

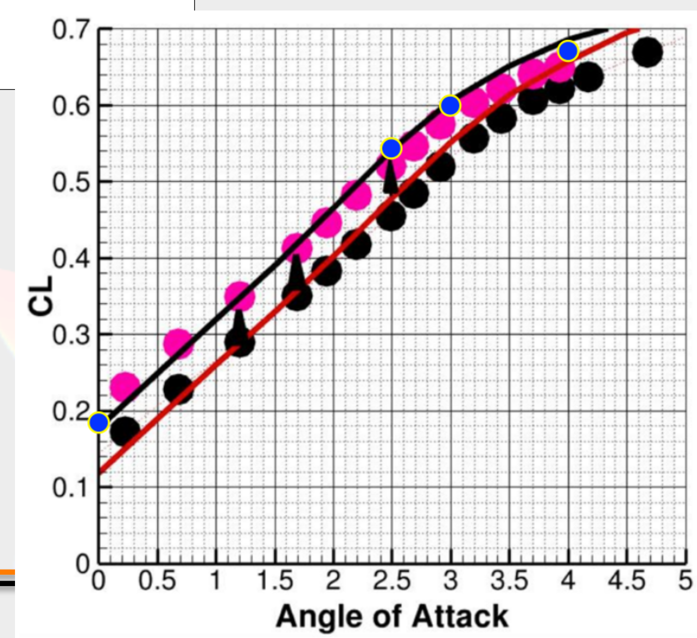

# Evolution Trajectory of CFD

**Flo107-MB → TFLO → SuMB** at Stanford University under ASCI program.

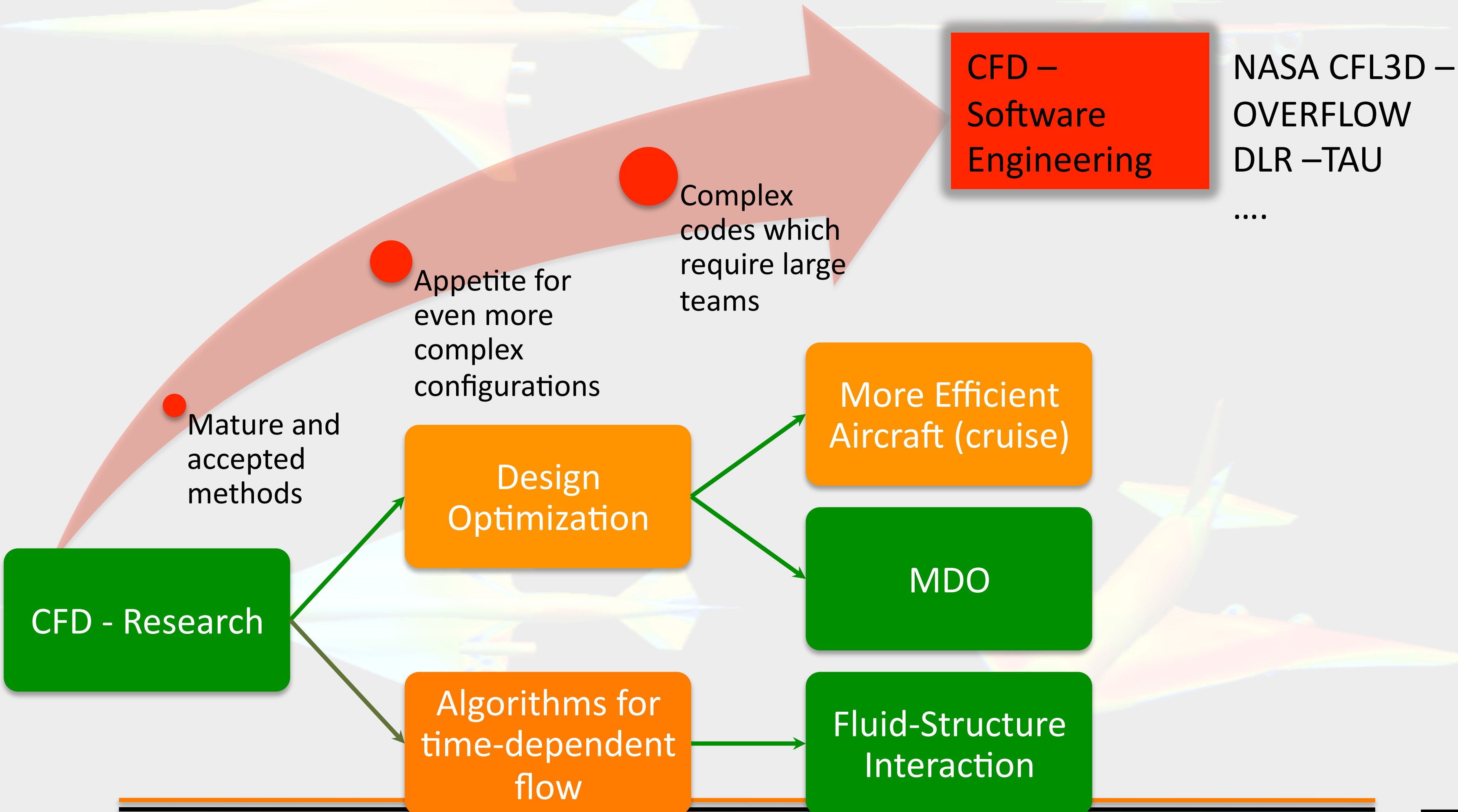

# Number of Design Variables is Large

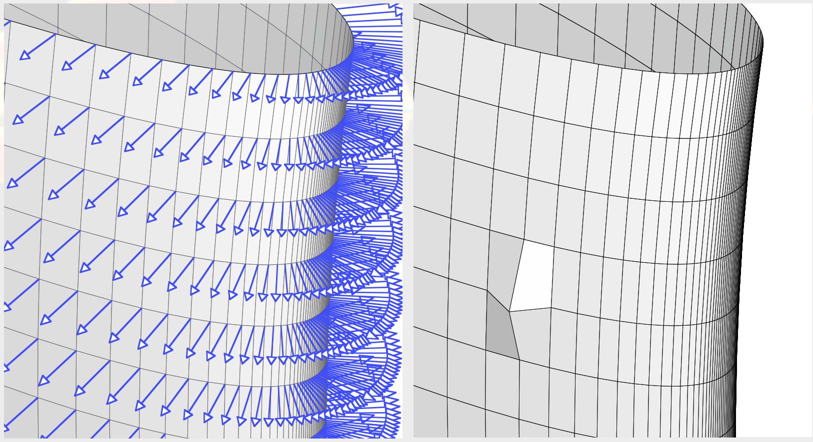

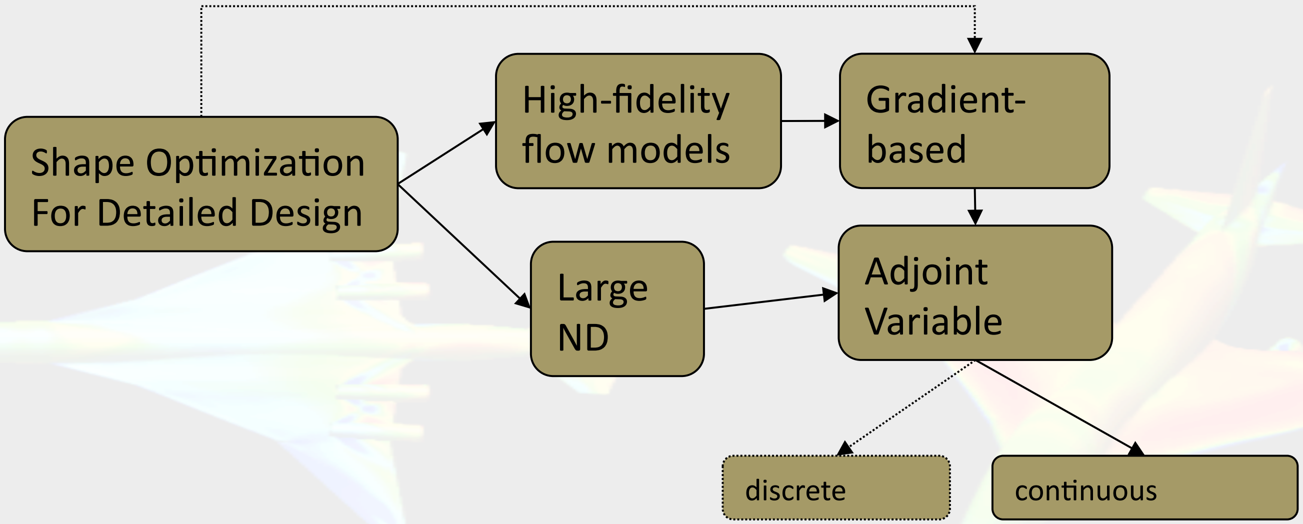

# Application of Control Theory

## GOAL : Drastic Reduction of the Computational Costs

***Drag Minimization*** ≡ ***Optimal Control of Flow Equations***
***<u>subject to</u> Shape(wing) Variations***

Define the cost function

$$I = I(w,F)$$

and a change in $F$ results in a change

$$\delta I = \left[\frac{\partial I}{\partial w}\right]^T \delta w + \left[\frac{\partial I}{\partial F}\right]^T \delta F$$

Suppose that the governing equation $R$ which expresses the dependencd of $w$ and $F$ as

$$R(w,F) = 0$$

and

$$\delta R = \left[\frac{\partial R}{\partial w}\right]\delta w + \left[\frac{\partial R}{\partial F}\right]\delta F = 0$$

# Application of Control Theory (Cont.)

Since the variation $\delta R$ is zero, it can be multiplied by a Lagrange Multiplier $\psi$ and subtracted from the variation $\delta I$ without changing the result.

$$\delta I = \frac{\partial I^T}{\partial w}\delta w + \frac{\partial I^T}{\partial F}\delta F - \psi^T\left(\left[\frac{\partial R}{\partial w}\right]\delta w + \left[\frac{\partial R}{\partial F}\right]\delta F\right)$$

$$= \left\{\frac{\partial I^T}{\partial w} - \psi^T\left[\frac{\partial R}{\partial w}\right]\right\}\delta w + \left\{\frac{\partial I^T}{\partial F} - \psi^T\left[\frac{\partial R}{\partial F}\right]\right\}\delta F$$

Choosing $\psi$ to satisfy the adjoint equation

(Adjoint)

$$\left[\frac{\partial R}{\partial w}\right]^T \psi = \frac{\partial I}{\partial w}$$

the first term is eliminated, and we find that

(Gradient)

$$\delta I = \left\{\frac{\partial I}{\partial F}^T - \psi^T\left[\frac{\partial R}{\partial F}\right]\right\}\delta F$$

**One Flow Solution + One Adjoint Solution**

# Adjoint – Viscous Terms

$$\frac{\partial F_{vi}}{\partial \xi_i} = \frac{\partial}{\partial \xi_i}\left(S_{ij} f_{vj}\right).$$

$$\int_{\mathcal{B}} \psi^T \left(\delta S_{2j} f_{vj} + S_{2j}\delta f_{vj}\right) d\mathcal{B}_\xi - \int_{\mathcal{D}} \frac{\partial \psi^T}{\partial \xi_i}\left(\delta S_{ij} f_{vj} + S_{ij}\delta f_{vj}\right) d\mathcal{D}_\xi,$$

$$\tilde{w}^T = (\rho, u_1, u_2, u_3, p)^T \qquad \delta w = M\delta\tilde{w}, \qquad \delta\tilde{w} = M^{-1}\delta w$$

$$\begin{aligned}
(\tilde{L}\psi)_1 &= -\frac{p}{\rho^2}\frac{\partial}{\partial \xi_l}\left(S_{lj}\kappa\frac{\partial \theta}{\partial x_j}\right)\\
(\tilde{L}\psi)_{i+1} &= \frac{\partial}{\partial \xi_l}\left\{S_{lj}\left[\mu\left(\frac{\partial \phi_i}{\partial x_j} + \frac{\partial \phi_j}{\partial x_i}\right) + \lambda\delta_{ij}\frac{\partial \phi_k}{\partial x_k}\right]\right\}\\
&+ \frac{\partial}{\partial \xi_l}\left\{S_{lj}\left[\mu\left(u_i\frac{\partial \theta}{\partial x_j} + u_j\frac{\partial \theta}{\partial x_i}\right) + \lambda\delta_{ij}u_k\frac{\partial \theta}{\partial x_k}\right]\right\} \qquad \text{for} \quad i = 1,2,3\\
&- \sigma_{ij}S_{lj}\frac{\partial \theta}{\partial \xi_l}\\
(\tilde{L}\psi)_5 &= \frac{1}{\rho}\frac{\partial}{\partial \xi_l}\left(S_{lj}\kappa\frac{\partial \theta}{\partial x_j}\right).
\end{aligned}$$

# The pinnacle of our efforts with Compressible RANS

- Solver based on my work with Antony 1984-1994
- Viscous Adjoint first successfully implemented in a coding blitz in the summer of 1995 (MDXX Project) together with Antony and and Niles Pierce  and refined over a decade.

Solvers for Viscous Flow

Finite Volume | Multi-grid Time-Stepping

Aero-Design Optimization

CFD Complements Wind Tunnel | Reduces Testing by 10-fold | Compressed Design cycle | Better Performance

Paradigm Shift In Aerodynamic Design

S Y N 1 0 7

# "A FINISHED THEORY? ARE YOU CRAZY? DON'T YOU WANT AN ACADEMIC CAREER?"
## Professor Marvin Bressler

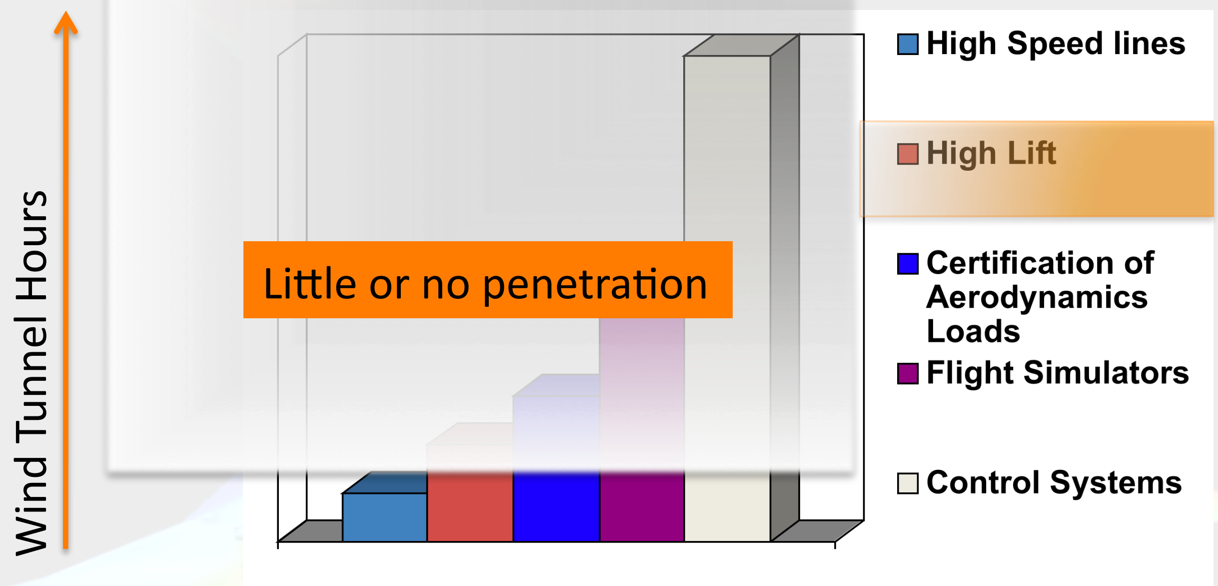

# Drag Minimization (High Lift)

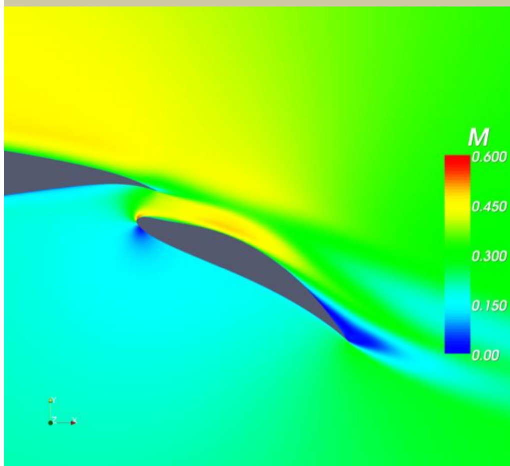


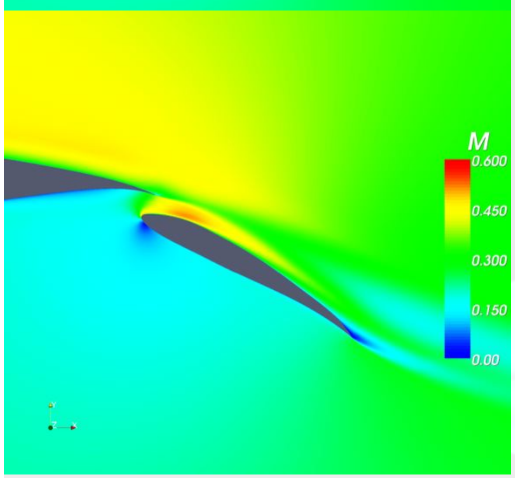


Arron Melvin , Ph.D. 2007

Three 448x64 blocks
321 points on each element
M = .15
Re= 8x10^6

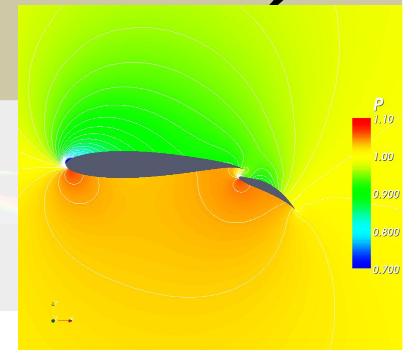

**K-T 30° FLAP**
**DESIGN SUMMARY**

| | $C_l$ | $C_d$ | % $C_d$ Reduction |
|---|---|---|---|
| Baseline | 2.2900 | 0.0591 | |
| Gap | 2.2908 | 0.0563 | 4.7 |
| Overlap | 2.2902 | 0.0591 | 0. |
| Gap & Overlap | 2.2930 | 0.0561 | 5.1 |
| Element 1 | 2.2939 | 0.0586 | 0.8 |
| Element 2 | 2.2905 | 0.0540 | 8.6 |
| Elements 1 & 2 | 2.2907 | 0.0533 | 9.8 |
| Element 1 & Gap,Overlap | 2.2945 | 0.0557 | 5.8 |
| Element 2 & Gap,Overlap | 2.2910 | 0.0539 | 8.8 |
| Elements 1,2 & Gap,Overlap | 2.2907 | 0.0526 | 11. |

# Drag Minimization Ground Effect

Arron Melvin , Ph.D. 2007
(won F1 – Championship with Brawn GP 2009)

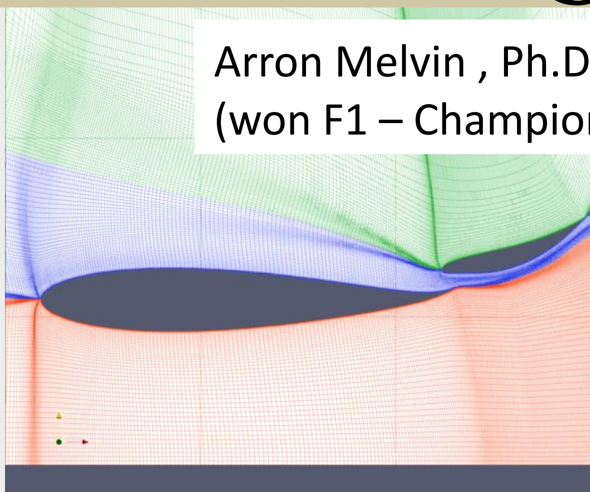

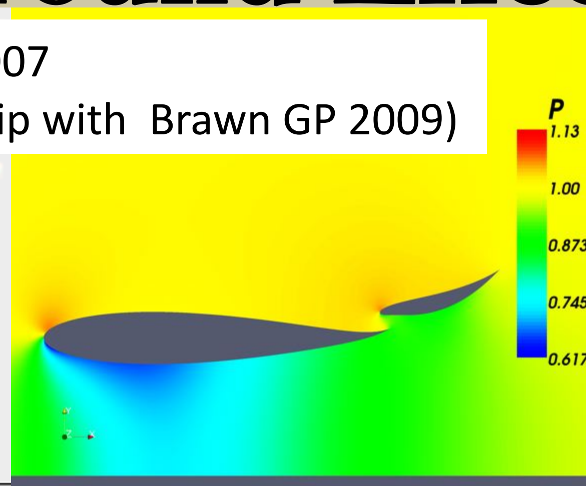


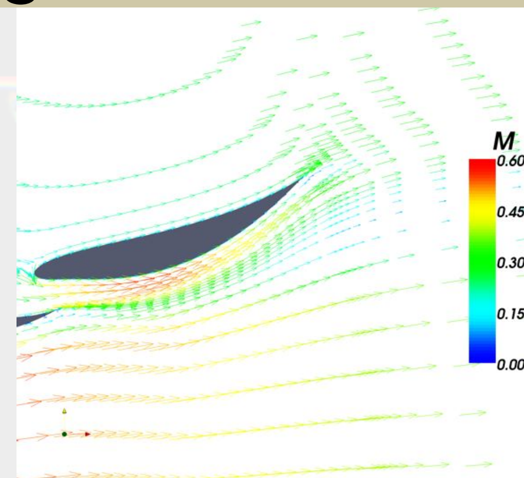


| | $C_l$ | $C_d$ | % $C_d$ Reduction |
|---|---|---|---|
| Baseline | -3.6980 | 0.0938 | |
| Gap & Overlap | -3.6978 | 0.0890 | 5.1 |
| Element 1 | -3.6982 | 0.0921 | 1.8 |
| Element 2 | -3.6980 | 0.0841 | 10. |
| Elements 1 & 2 | -3.6982 | 0.0825 | 12. |
| Element 2 & Gap,Overlap | -3.6979 | 0.0787 | 16. |
| Elements 1,2 & Gap,Overlap | -3.6981 | 0.0759 | 19. |

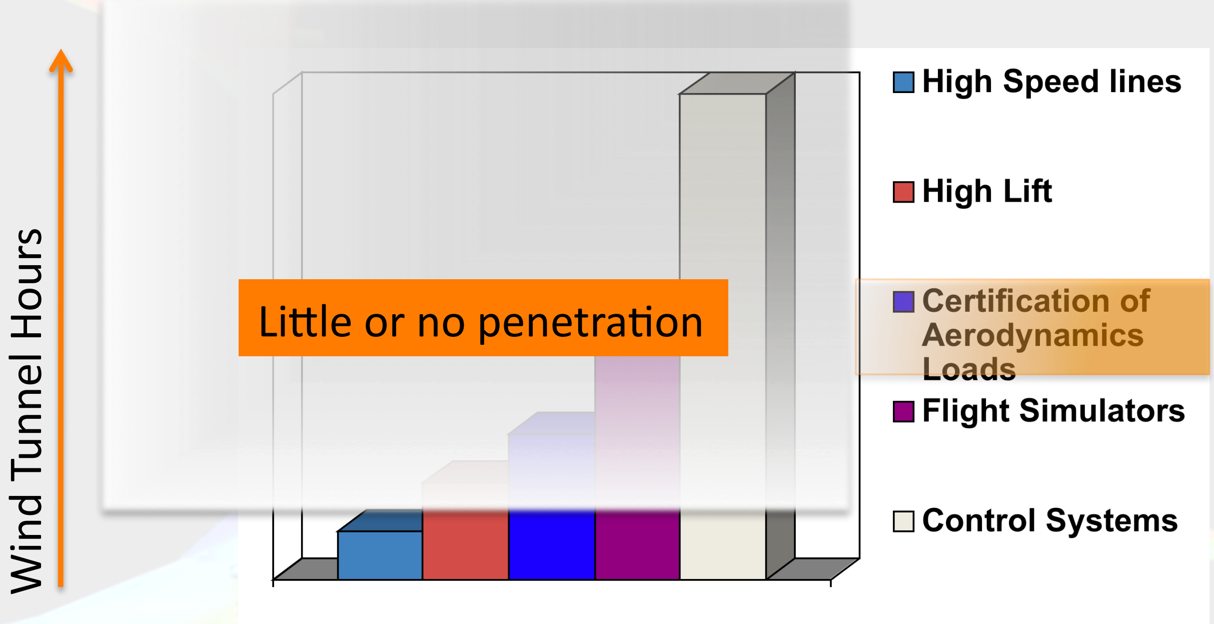

Wind Tunnel Hours
Little or no penetration
High Speed lines
High Lift
Certification of Aerodynamics Loads
Flight Simulators
Control Systems

# UQ – Iced Airfoils

## Computational cost

- Full 3D simulations require $\sim$ 200 CPU hours for a polar, making large numbers of 3D icing studies unfeasible.
- Wing icing tends to be largely 2D, where airfoils require $\sim$ 1000 seconds to compute a polar.
- With a $\sim$\$1300 commodity desktop with a 16-core processor, we can run high fidelity simulations on 42,000 geometries in one month.

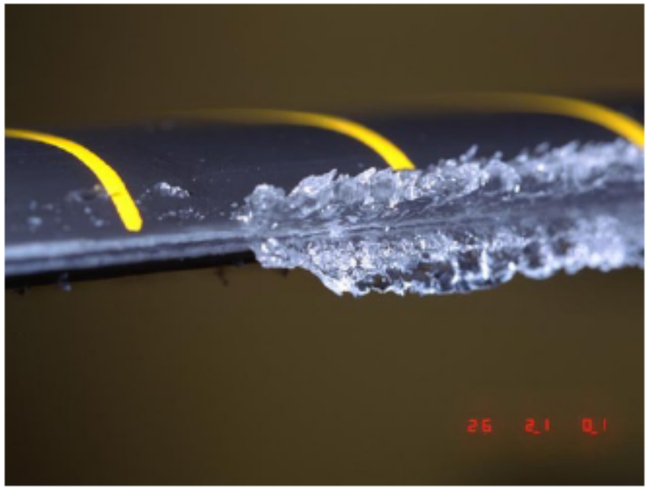

Figure: Wing icing, NASA Glenn

# Iced Airfoils

## Comparison with experimental work

- Using ice geometries generated by LEWICE, Papadakis et al (AIAA 2001) tested ice effects on 2D wing sections.
- Base geometry from NASA Glenn's DHC-6 icing research aircraft tail section (NACA $63_A213$) at $M_\infty = 0.21$, $Re = 4,000,000$.
- Horn sizes are 1.2% and 2.5% of chord.

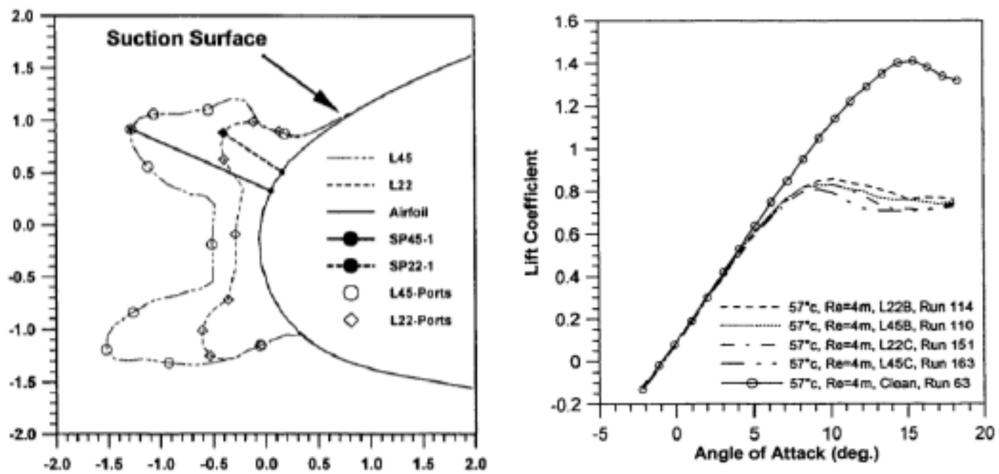


Figure: Papadakis (2001)

# Iced Airfoils - Validation

- Small changes to the geometry can lead to large flowfield changes.
- At the same flight conditions, the clean wing exhibits fully attached flow, while the iced wings are fully separated.

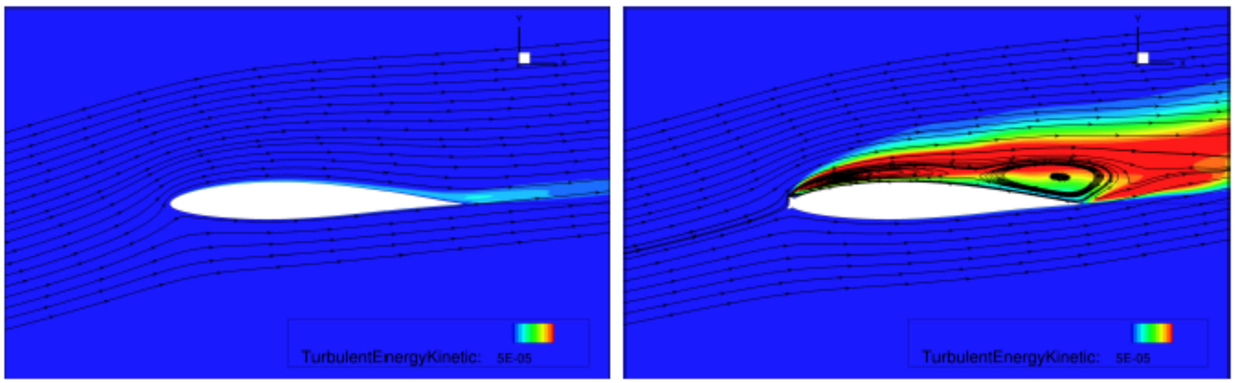


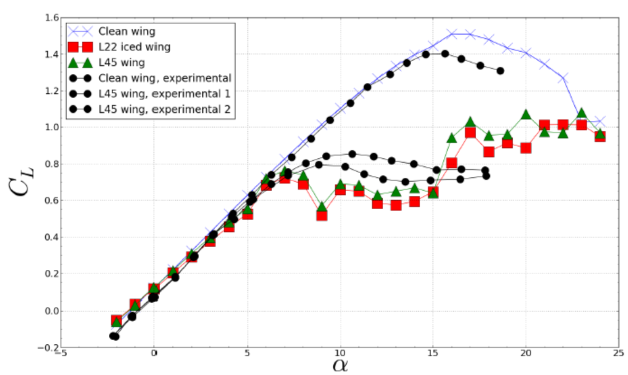


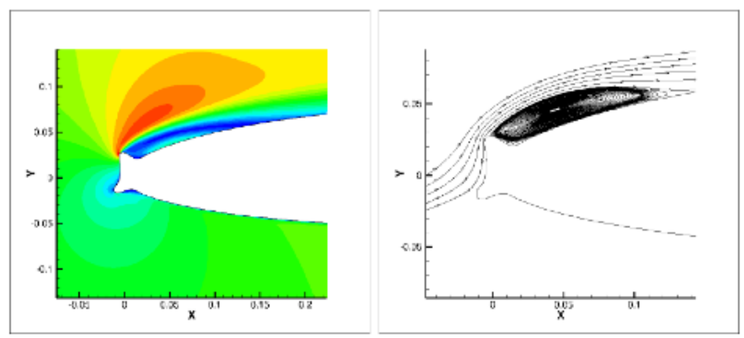


(a) The Mach number flow field at an AoA of 9°.

(b) Flow streamlines forming a separation bubble, at an AoA of 9°.

# UQ – Montecarlo Method
# A. Beebe and E. Meland Senior Project

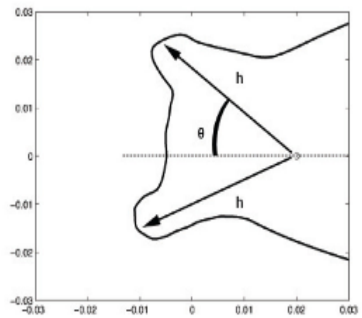


Figure 2.2: The geometric horn ice parameters.

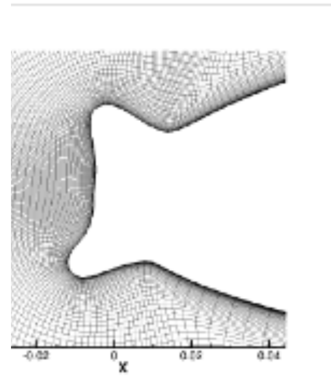

(a)

(b)

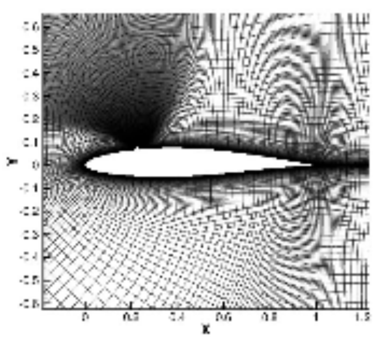

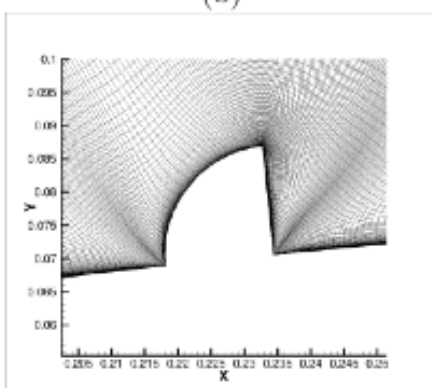

(c)

(d)

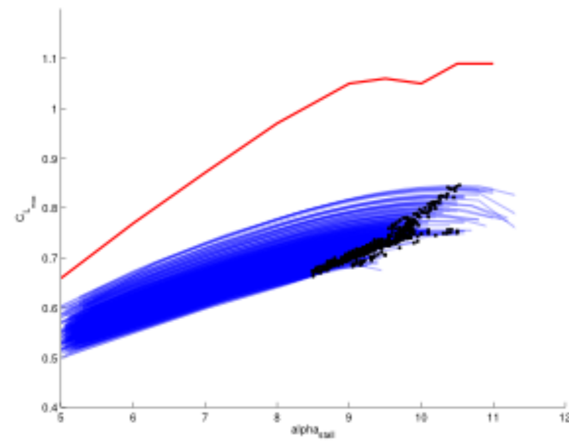

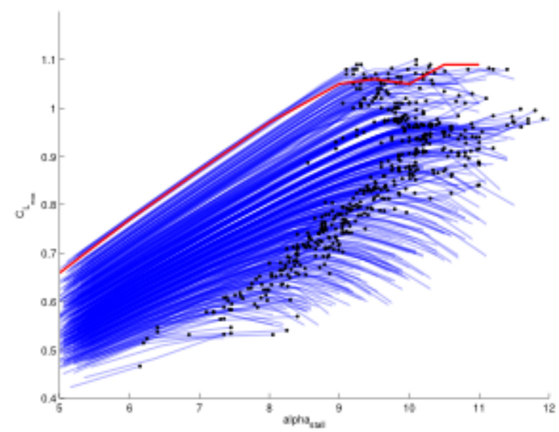

# Ridge – Results for several Bi-variate Distributions

Output for 9 different Bivariate distributions

Mean location 20% c
Mean radius 1.4% c

4,500 polar
10 angles of attack per polar

Fast solvers make this kind of Statistical analysis feasible.

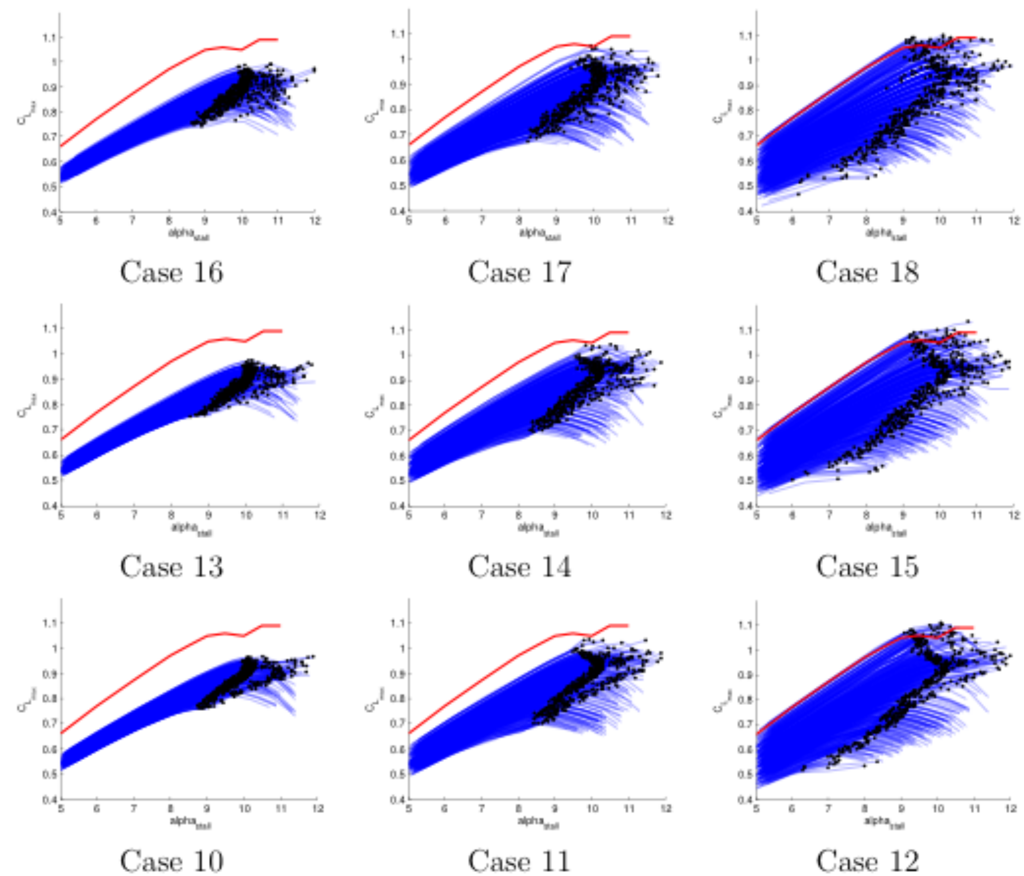


Figure A.4: $C_L$ vs $\alpha$ curves for the 9 ridge ice studies. Clean airfoil denoted by red, $C_{L_{max}}$ denoted by black dot.

# Ancillary Applications (Solver)

- Ship Hydrodynamics

Calculations performed with G. Cowles (Ph.D ‘01)
In Support to the successful Alinghi 2003 Challenge

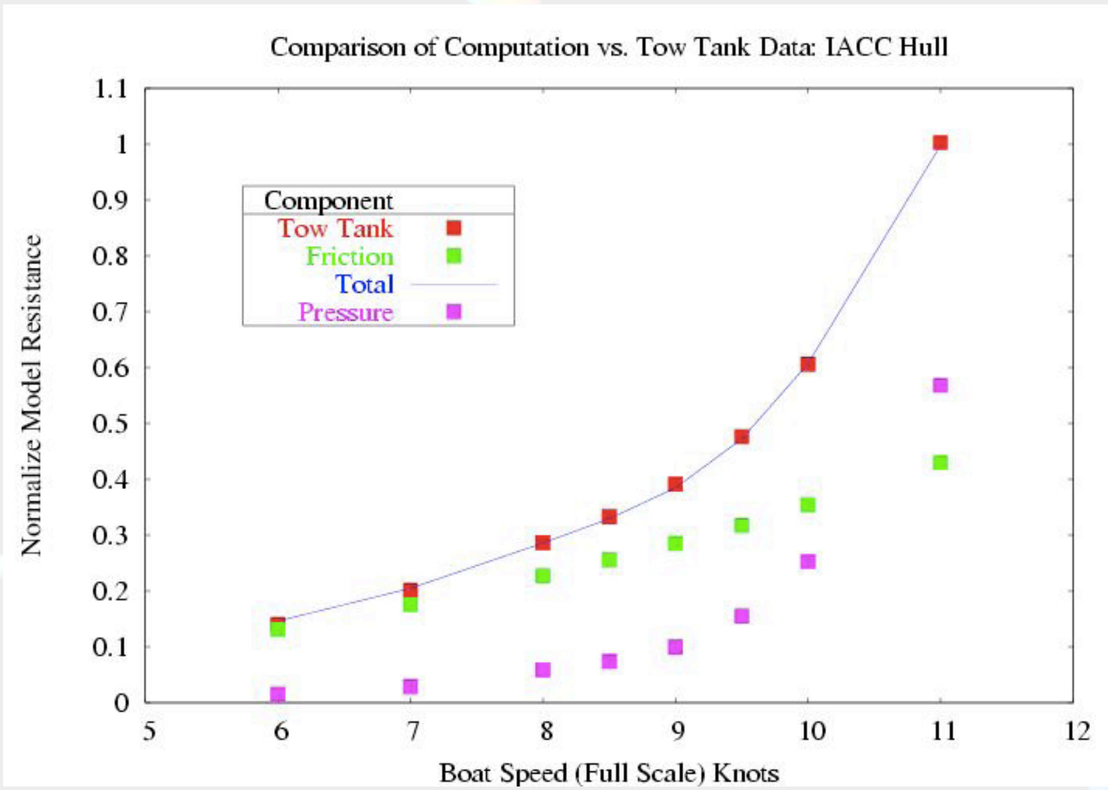


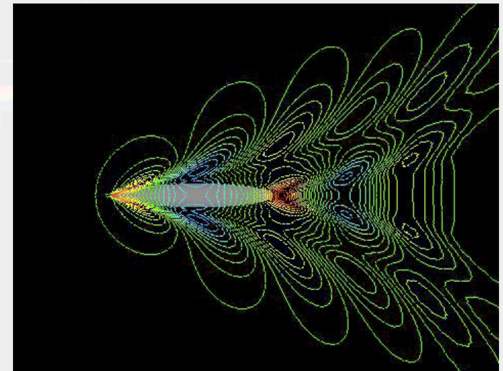

# Ancillary Applications(Opt.)

Ph.D. J. Dreyer – Penn State

- Inverse Design of Impellers (Pumps/Propulsion)

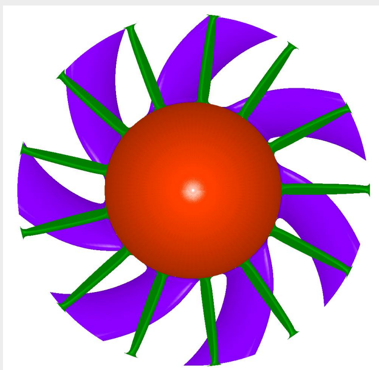

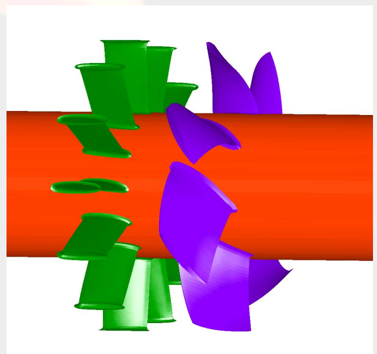

**HI**gh **RE**ynolds number axial flow **P**ump test facility at ARL Penn State

2 blade rows: IGV (13), Rotor (7)

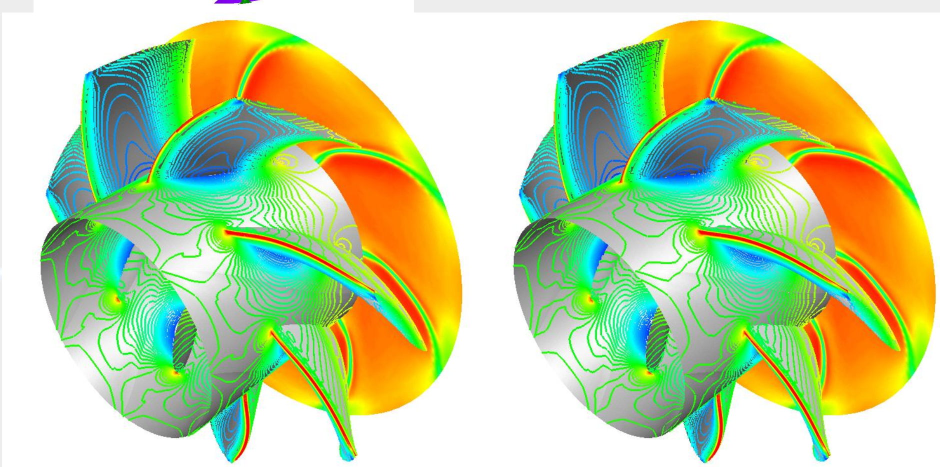

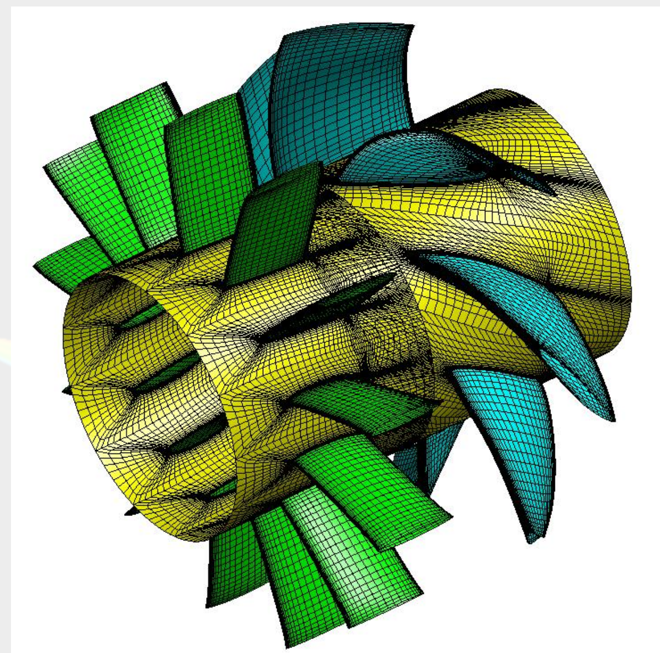

# Ancillary Applications(Opt.)

- Inverse Design of Impellers (Pumps/Propulsion)

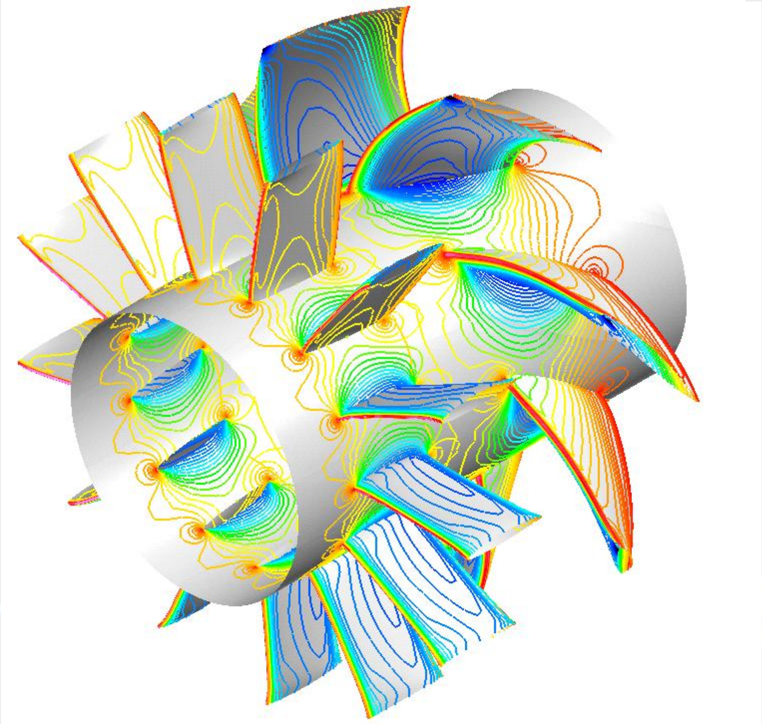

DESIGN

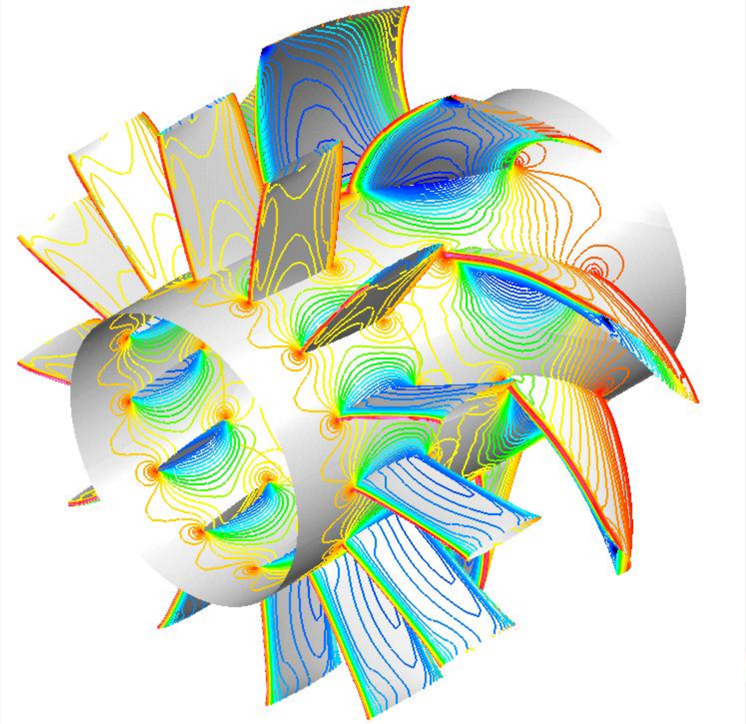

TARGET

# Ancillary Applications(Opt.)

## Low Cavitation Foils

At right:
Computed cavitation bucket for a NACA 65410 blade section

### Pathology of a cavitation "bucket"

"Floor" of bucket (b.) surrounded by steep sides (a. & c.)

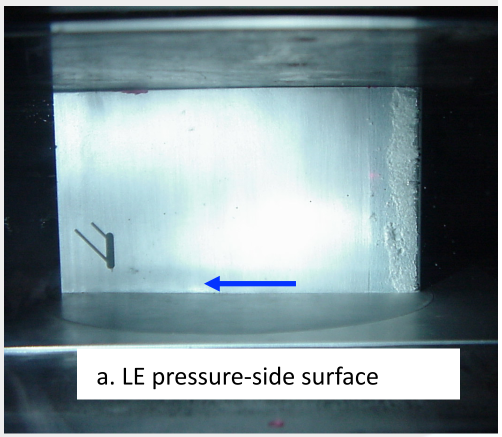
a. LE pressure-side surface

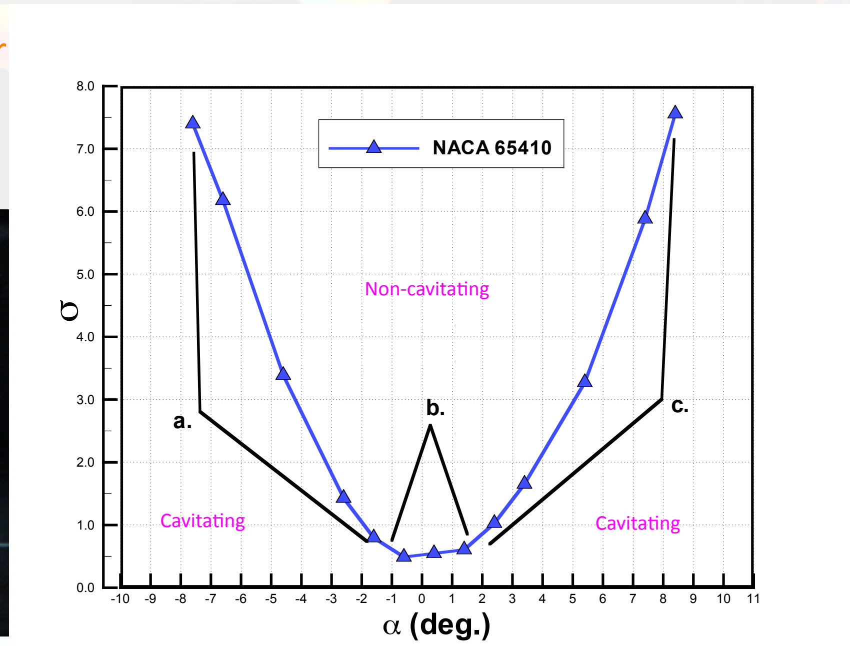


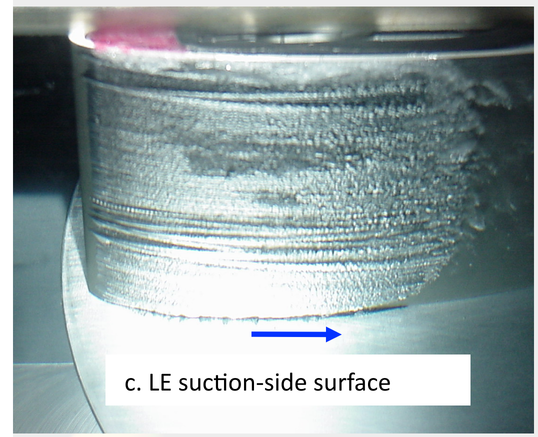
c. LE suction-side surface

Floor is due to benign suction face pressure distribution

Steep sides are due to the formation of LE suction peaks

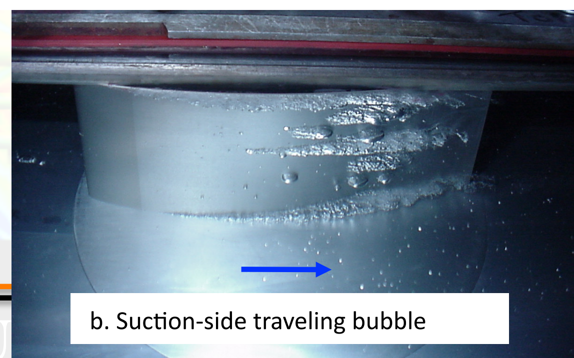
b. Suction-side traveling bubble

Objective:
For a given blade section, increase the width of the floor and, if possible, decrease the steepness of the sides

# Low Cavitation Foil

*Reduction of Problematic Suction Peaks*

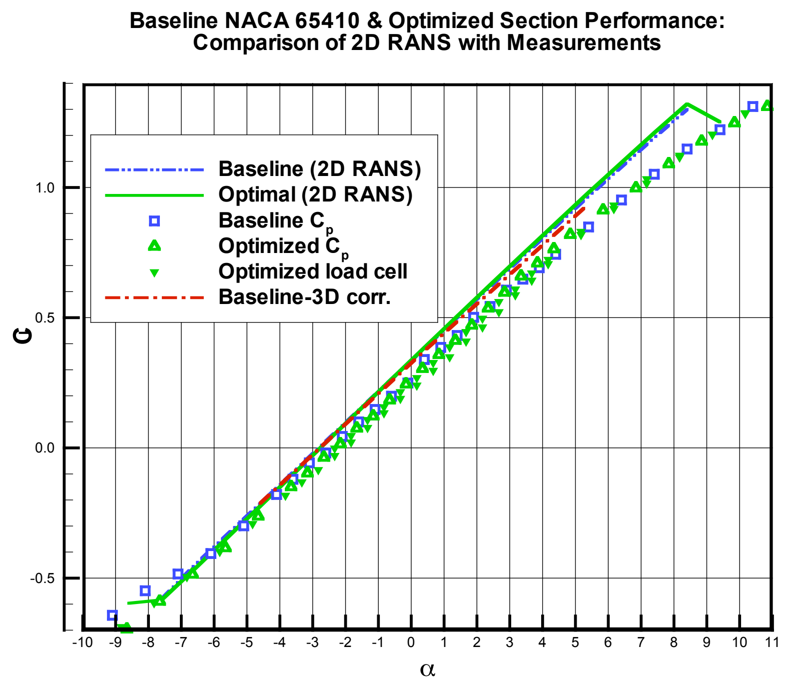


*Minimization of Axial Force*

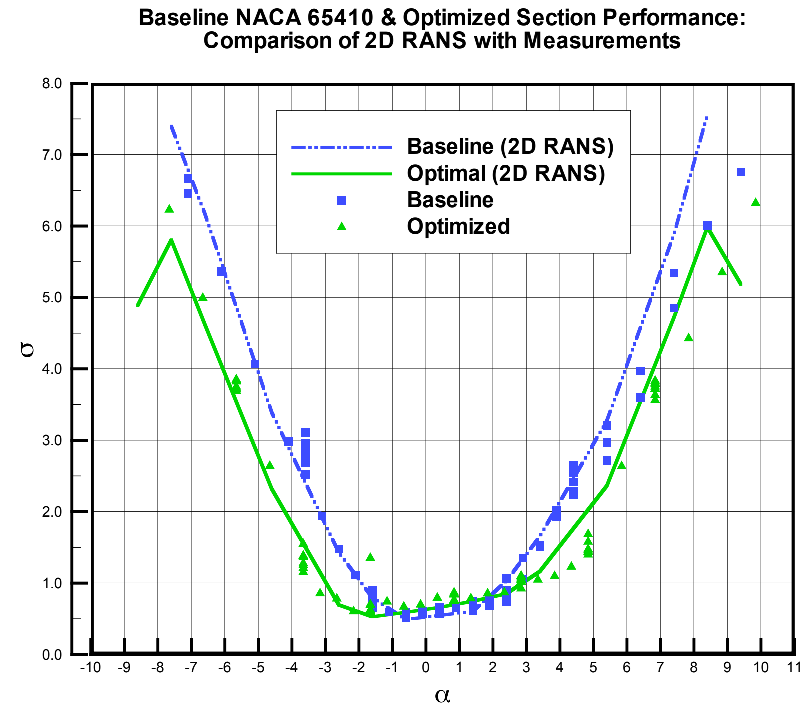


PRINCETON UNIVERSITY

# VAWT simulation basics

- Advantages over horizontal axis:
  - Independent of wind direction
  - Closer packing in wind farms
  - Easier maintenance
  - Low noise
  - Potential scaling benefits
- Disadvantages:
  - Dynamic stall problems
  - Difficulty in start-up
- Aerodynamic challenges:
  - Retreating blade stall (loss of power)
  - Turbulent wake interaction (fatigue)
  - Interaction with the ABL

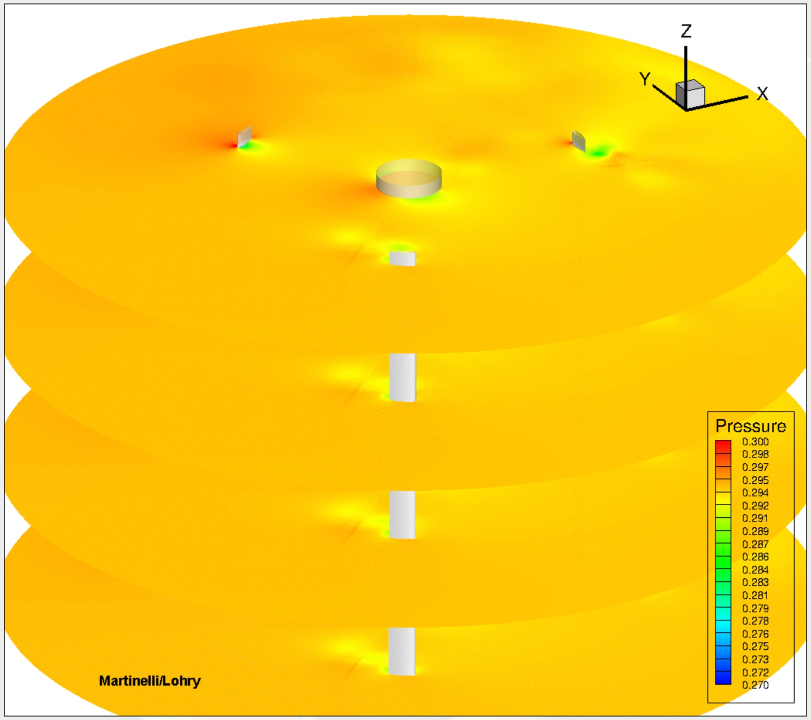


– Menter's SST Turbulence Model, 5 Million grid points.
– About 256 CPU-hours per revolution – 10 times faster than industrial CFD codes.

# Retreating blade stall

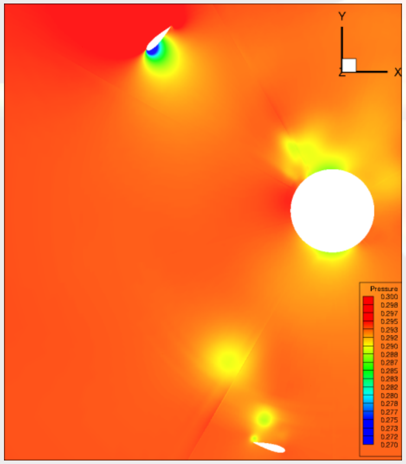

t=0

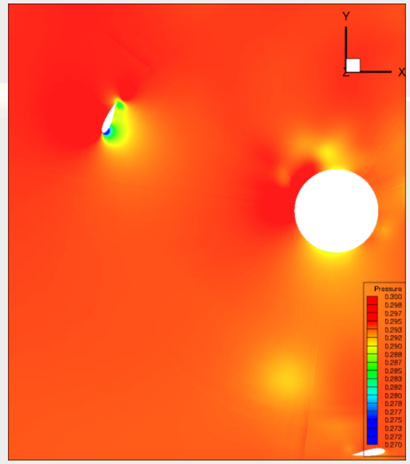

t=0.13s

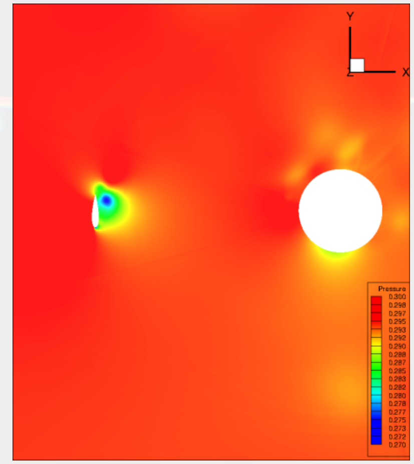

t=0.26s

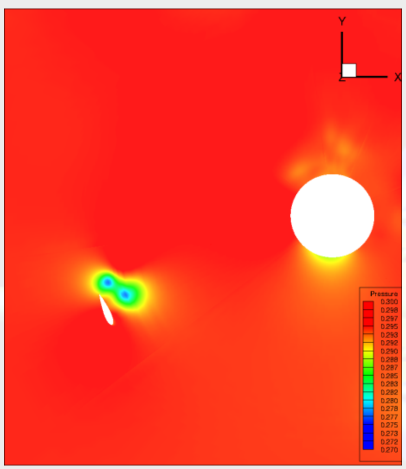

t=0.38s

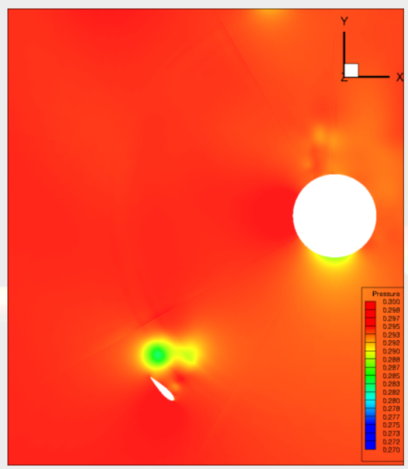

t=0.51s

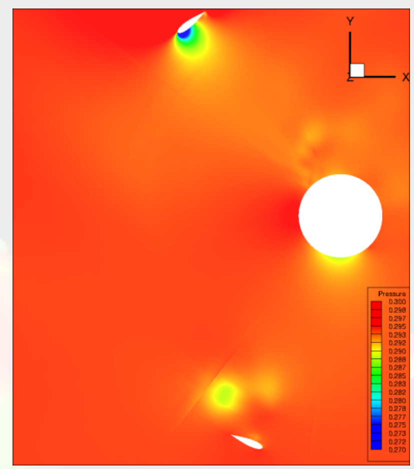

t=0.64s

# ISO-SURFACES PRESS. LOSSES

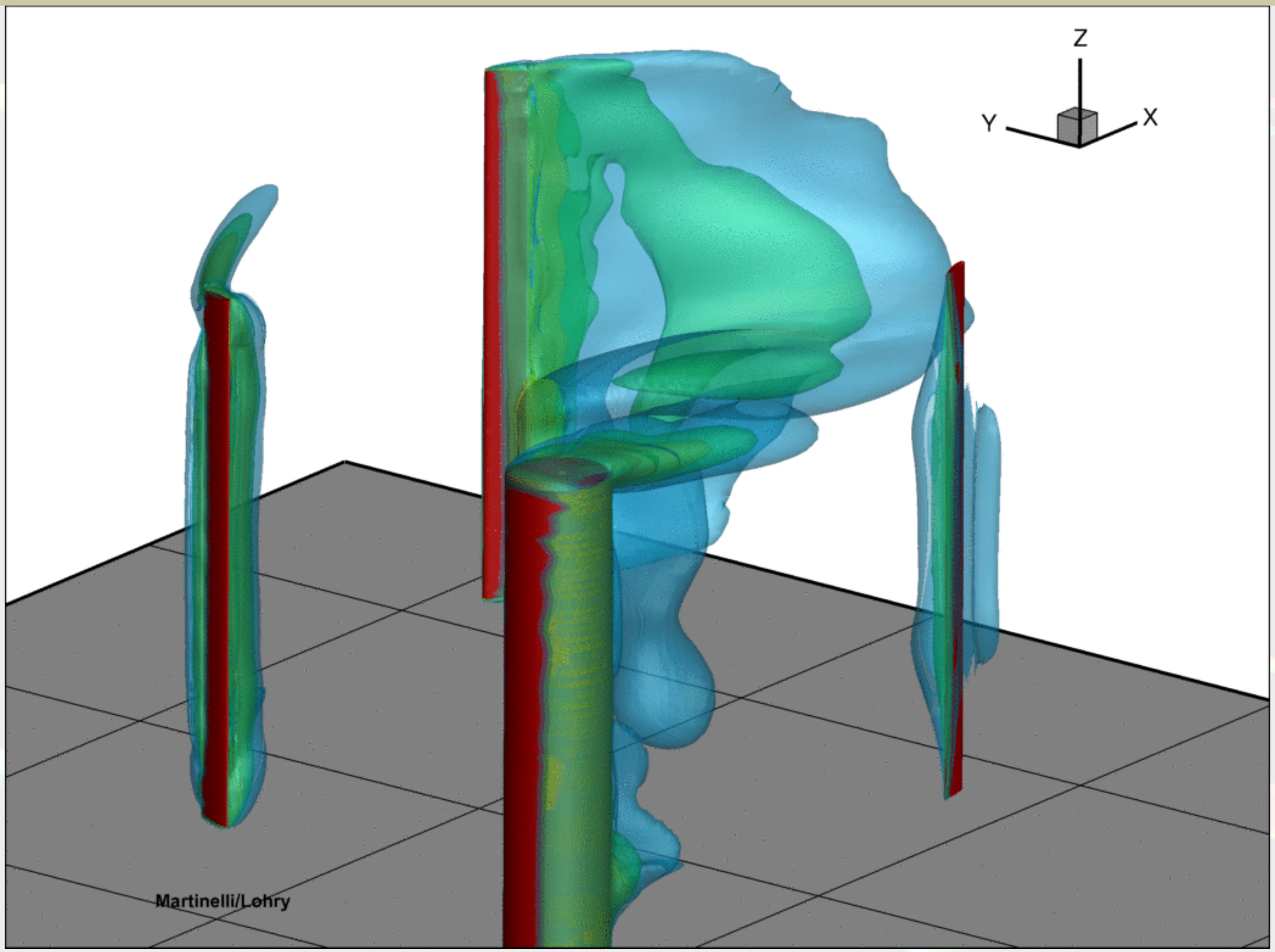


Avg. Wind Speed : 5.7m/s R.P.M. : 12

# Current Research Thrust

Object Oriented rewrite of software for ease of code maintenance.

Improve upon the simulation capabilities for problems with large mesh deformation
(i.e. fluid-structure interaction problems)

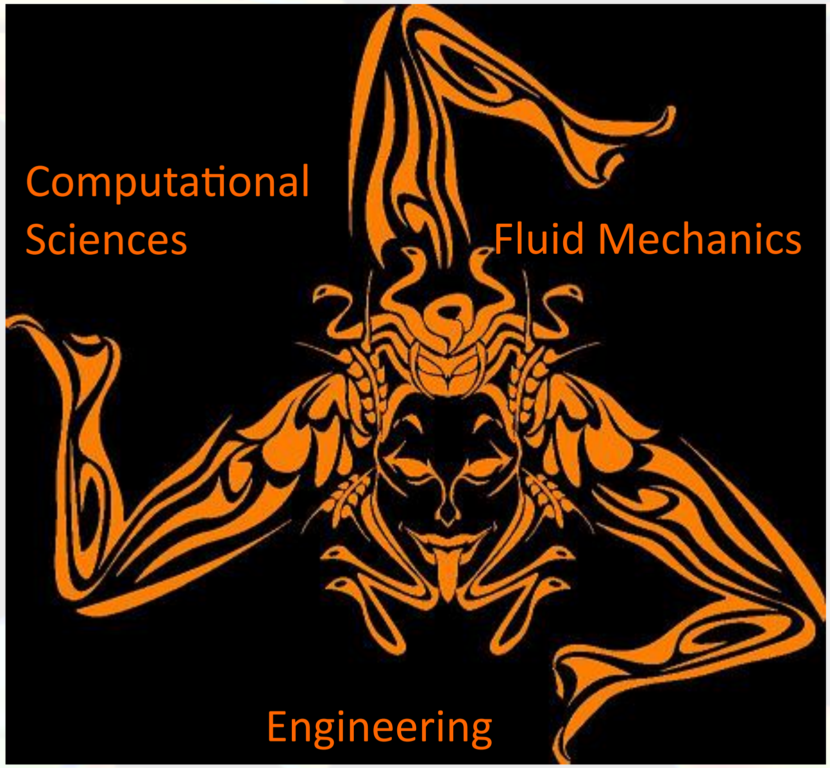


Improve Modeling of Separated flow

URANS + DES

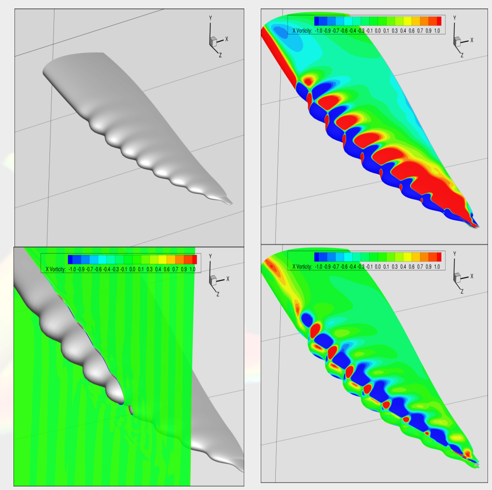

Design Optimization for Control/Mitigation of Separated Flow